Energy Engineering

Tech Science Press

DOI: 10.32604/ee.2024.043294

ARTICLE

Optimal Bidding Strategies of Microgrid with Demand Side Management for Economic Emission Dispatch Incorporating Uncertainty and Outage of Renewable Energy Sources

Mousumi Basu[1], Chitralekha Jena[2], Baseem Khan[3,4,*] and Ahmed Ali[4]

[1]Department of Power Engineering, Jadavpur University, Jadavpur, India

[2]School of Electrical Engineering, KIIT University, Bhubaneswar, India

[3]Department of Electrical and Computer Engineering, Hawassa University, Hawassa, Ethiopia

[4]Department of Electrical and Electronic Engineering Technology, Faculty of Engineering and the Built Environment, University of Johannesburg, Johannesburg, South Africa

[*]Corresponding Author: Baseem Khan. Email: baseemkh@hu.edu.et

Received: 06 June 2023 Accepted: 28 November 2023 Published: 26 March 2024

ABSTRACT

In the restructured electricity market, microgrid (MG), with the incorporation of smart grid technologies, distributed energy resources (DERs), a pumped-storage-hydraulic (PSH) unit, and a demand response program (DRP), is a smarter and more reliable electricity provider. DER consists of gas turbines and renewable energy sources such as photovoltaic systems and wind turbines. Better bidding strategies, prepared by MG operators, decrease the electricity cost and emissions from upstream grid and conventional and renewable energy sources (RES). But it is inefficient due to the very high sporadic characteristics of RES and the very high outage rate. To solve these issues, this study suggests non-dominated sorting genetic algorithm II (NSGA-II) for an optimal bidding strategy considering pumped hydroelectric energy storage and DRP based on outage conditions and uncertainties of renewable energy sources. The uncertainty related to solar and wind units is modeled using lognormal and Weibull probability distributions. TOU-based DRP is used, especially considering the time of outages along with the time of peak loads and prices, to enhance the reliability of MG and reduce costs and emissions.

KEYWORDS

Micro-grid; distributed energy resources; demand response program; uncertainty; outage

Nomenclature

PSP	Pumped storage plant
F_C	Cost function
F_E	Emission function
a_{Gi}, b_{Gi}, c_{Gi}	Cost coefficients of ith gas turbine
$\alpha_{Gi}, \beta_{Gi}, \gamma_{Gi}$	Emission coefficients of ith gas turbine
UR_i, DR_i	Upper and lower ramp limits of ith gas turbine
P_{Git}	Output of ith gas turbine
P_{Gi}^{min}, P_{Gi}^{max}	Min[m] and Max[m] limit of generation for ith gas turbine
$P_{grid,t}$	Power procured from upstream grid at time t

P_{grid}^{max}	Maximum power exchange between MG and upstream grid
$cgrid_t$	Grid electricity price at time t
$egrid_t$	Emission of grid power at time t
P_{wjt}	Wind power available of jth wind turbine at time t
P_{wj}^{min}, P_{wj}^{max}	Min^m and Max^m generation limits for jth wind turbine
P_{wrj}	Wind power rated of jth wind turbine
d_{wj}	Direct cost coefficient for the jth wind turbine
v_{in}	Cut- in velocity of wind
v_{out}	Cut-out velocity of wind
v_r	Velocity of rated wind
v_{wt}	Forecasted velocity of wind
α, β	Scale and shape factors for Weibull PDFs
μ_{Log}, σ_{Log}	Lognormal PDF's standard deviation and mean
$\mu_{Norm}, \sigma_{Norm}$	Standard deviation of the mean and variance
P_{PVkt}	Power output from kth PV plant
P_{srk}	Equivalent rated power output of the PV plant
G	Forecast of radiation of solar
G_{std}	Radiation from the sun in a normal environment
R_c	Specific level of radiation
d_{PVk}	Direct cost co-efficient for the kth solar PV plant
u_{wj}, o_{wj}	Penalty and reserve cost for the jth wind turbine
u_{PVk}, o_{PVk}	Penalty and reserve cost for the kth PV plant
P_{ghlt}	Generated power of lth PSP at time t
P_{phlt}	Pumping power of lth PSP
P_{ghl}^{min}, P_{ghl}^{max}	Min^m and max^m generation power limits of lth PSP
P_{phl}^{min}, P_{phl}^{max}	Min^m and max^m pumping power limits of lth PSP
$Q_{ghlt}\left(P_{ghlt}\right)$	Discharge rate of lth PSP
$Q_{phlt}\left(P_{phlt}\right)$	Pumping rate of lth PSP
$Q_{spent,TOT,l}$	Total amount of water spent for generation of lth PSP
$Q_{pump,TOT,l}$	Total amount of water pumped of lth PSP
$Q_{net,spent,l}$	Net amount of water spent by lth pumped storage hydraulic unit during operation cycle
$V_{res,lt}$	Volume of water in upper reservoir of lth PSP
$V_{res,l}^{min}$, $V_{res,l}^{max}$	Min^m and max^m limits of upper reservoir storage of lth PSP
$V_{res,l}^{start}$, $V_{res,l}^{end}$	Specified volume of water at starting and final in upper reservoir of lth PSP
Inc^{max}	Max^m increased load at any hour (MW)
$L_{Base,t}$	Forecasted base load
DR_t	Percentage of forecasted based load participated in DRP
DR^{max}	Limit on how much of the base load can participate in DRP
Inc_t	Amount of increased load
Ls_t	Shiftable load
F	Failure rate (failure times/year)
F_{PV}, F_w	Wind and solar power system's maximum failure rate (failure times/hour)
$MTTR$	Mean time to repair
MDT_i, MUT_i	Mean down and up time of ith gas turbine
ρ	Rate of forced outage

$\rho_{Repair}, \rho_{Aging}, \rho_{Weather}$	Forced outage rate due to repairable, aging, and weather dependent failure
ρ_{wjt}, ρ_{PVkt}	At time t, forced outage rate of jth wind turbine and kth solar power plant
λ	Probability of failure
S_{wjt}	'1' if jth wind power unit is scheduled on at time t and otherwise '0'
S_{PVkt}	'1' if k th Solar PV plant is scheduled at time t and otherwise '0'
S_{Gjt}	'1' if ith gas turbine is scheduled on at time t and otherwise '0'
$T_{on,i,(t-1)}, T_{off,i,(t-1)}$	On and off condition of ith gas turbine before $(t-1)$th time
t, T	Time index and scheduling period
T_{gen}	Set containing time intervals where PSP operate in generation mode
T_{pump}	Set containing time intervals where PSP operate in pumping mode
N_G	No. of thermal generating units
N_w	No. of wind turbine
N_{PV}	No. of solar PV plant
N_{Pump}	No. of PSP

1 Introduction

When it comes to a smart grid, the most important component is the microgrid (MG), which provides an efficient energy system with better power quality, reliability, and economics to grid-independent end-user locations. As smart grid technology advances, MGs must continue to function with a very well-pumped-storage-hydraulic (PSH) unit and increase customer engagement through demand-side management [1,2]. Thus, MG can purchase power from upstream grid-connected, distributed energy sources with the advantage of time-varying electricity prices to meet its demand. When it comes to renewable energy, though, there are several issues that make it difficult for MG operators to purchase power from day-ahead markets at variable prices so that costs and pollution may be reduced concurrently. Hence, to bid for electricity in the day-ahead market, MG should plan an optimal bidding strategy to buy power from the upstream grid with a demand response program (DRP), taking into consideration the uncertainty and outages of the sources of renewable energy.

The best bidding strategy has been studied in the below mentioned references in order to reduce energy prices in the deregulated electricity market and to improve the dependability of the power system. Optimal Control of a Microgrid with Distributed Renewable Generation and Battery Energy Storage is presented in reference [3]. Stochastic programming and two-stage stochastic programming [4] have been used to design a bidding strategy for MG that maximizes both power scheduling and profit maximization [5]. A bi-level programming-based energy bidding strategy for MG has been proffered in reference [6], in which a stochastic model of uncertain renewable energy sources and loads is considered. A integrated demand response in multi-energy microgrids using deep reinforcement learning is presented in reference [7]. In reference [8], a day-ahead bidding strategy for grid-tied residential MG has been proposed. A robust optimization-based day-ahead bidding approach has been employed in reference [9] for maximizing the profit from the joint energy and spinning reserve markets. In reference [10], DRP is introduced in the bidding operation of MG to facilitate customers with active participation with the MG aggregator and system operator. Small-scale MGs are involved in a DRP-assisted real-time balancing bidding process in a hierarchical market model [11]. Another DRP-aided short-term bidding framework for MG has been represented in reference [12] as a robust optimization-based best-cost model.

The gas turbine discharges many pollutants, like SOx, NOx, and CO_2, into the atmosphere for electric utilities. The ambiance of reducing greenhouse gases is one of the important concerns. The

Clean Air Act of 1990 was intended to reduce greenhouse gases and acid rain. So for that, the gas turbine must decrease its sulfur oxide (SOx) and NOx levels of emission [13]. Today's society is looking for a secure and reliable source of energy that is both cost-effective and environmentally friendly.

1.1 Literature Review

A variety of tactics are suggested to decrease ambient greenhouse gases [14]. Dispatching, considering emissions, is preferable among these.

On the basis of historical data and a list, concerns about renewable energy resources (RER) are simulated. Bidding tactics in references [10–12] include demand response programs (DRPs) to relieve load only during times of high demand or high cost. DRP integration, on the other hand, may significantly improve the MG's dependability and operating costs during DER outages.

Based on economic environmental dispatch (EED) with DRP, this study proposes an efficient bid for MG based on the outages of intermittent renewable energy sources [15,16]. Wind turbine (WT) units use the Weibull PDF (WPDF), whereas solar photovoltaic (PV) units use the well-established Lognormal PDF (LPDF). These PDFs are widely used to estimate renewable energy sources' uncertainty probabilities. Within the anticipated upper and lower limits [17], all of the potential scenarios are mapped with repetition. To encourage MG to make precise decisions on power generation dispatch during bidding, penalty costs for underestimates and reserve costs for overestimations of RER outputs are included in the primary costs [16]. Forced outages are more likely to occur due to RER facilities' remoteness and difficult operating conditions. RER unit outage probability also follows certain mathematical formulations or PDFs based on distinct types of failures, such as repairable, aging, and weather-related [18–25]. References [26,27] discussed the economic dispatch problem using different computationally intelligent techniques. Considering the uncertainty and outage modeling of RERs, the MG operator performs the EED to settle the optimal power dispatch schedules of generators and pumped-storage-hydraulic (PSH) units and electricity purchasing in the day-ahead market to facilitate its bidding optimization. Here, NSGA-II is suggested to solve the EED problem. The techno-economic evaluation of combined power-to-hydrogen technology and hydrogen storage in an optimal bidding approach for microgrids with high penetration rates of renewable energy units was proposed by the authors in reference [28]. A grid-connected multi-microgrid system's ideal heat and power energy management, taking demand response and bidding strategy into account, was suggested by authors in reference [29] as an economic-environmental risk-averse approach. The coordinated optimal bidding techniques of aggregated microgrids were devised by the authors in reference [30]. In order to do this, demand-side management based on game theory is applied in an environment where electricity is sold. A clever predict-and-optimize framework for the bidding strategy of microgrids in a day-ahead electricity market was proposed by the authors in reference [31]. The effect of the ideal pump storage unit size on microgrid operational costs and energy market bidding was examined by the authors in reference [32]. The effect of the ideal pump storage unit size on microgrid running costs and energy market bidding was examined by authors in reference [33].

1.2 Research Gaps

Based on the review performed in the previous section, it is concluded that the previous researchers did not incorporate the emission constraints into the economic dispatch problem. Moreover, most of the researchers did not consider the demand-side management response. At last, various researchers did not consider the uncertainty and outages of renewable energy sources.

1.3 Contribution

To address the research gaps discussed in the previous subsection, the authors have made the following contributions to this manuscript:

1. Optimal bidding strategies for microgrids with demand-side management are presented.
2. Economic dispatch is proposed by incorporating uncertainty and outages from renewable energy sources.
3. Emission constraints are incorporated into the economic dispatch.
4. The non-dominated sorting genetic algorithm II (NSGA-II) is utilized for economic emission dispatch.

1.4 Organization of the Manuscript

The organization of the manuscript is as follows: Section two presents the problem formulation. Section three presents the proposed methodology. Section four presents the results and discusses them, followed by the conclusion.

2 Problem Formulation

The proposed MG is considered to be grid-connected and consists of gas turbines (GTs), a solar PV plant, wind power generation units, a pumped-storage-hydraulic (PSH) unit, and loads. Day-ahead weather data and electricity prices are assumed to be known from historical data and other factors. The MG operator must determine the degree of energy purchase from the upstream grid and GTs, solar PV plant, wind turbine, and PSH production in order to minimize overall cost and emissions simultaneously while taking into account associated constraints. For the sake of problem formulation, the following objective functions with constraints were used.

2.1 Modelling of the System

2.1.1 Arrangement of Probability of Solar Power Plant and Wind Turbine

Because of its unpredictability and intermittent nature, integrating solar power and wind turbines into an MG is difficult. MG's steady state security is imbalanced if demand spikes because of an underestimation of renewable power and an overestimation of its reserve capacity buffers, which wastes extra energy. MG's overall production and operating costs in energy bid planning are impacted by each of these factors. The use of probability distribution functions (PDFs), such as lognormal and Weibull, to assess penalty costs for underestimates and reserve costs for underestimates has led to a wide range of uncertainty models, such as beta, gumbel, and lognormal. The results of Eqs. (1) and (2) are well-followed by lognormal or Weibull PDFs [16].

$$f_G(G) = \frac{1}{G \times \sigma_{Log} \times \sqrt{2 \times \Pi}} \times e^{-\left\{\frac{-\left(\ln G - \mu_{Log}\right)^2}{2 \times \mu_{Log}{}^2}\right\}} \text{ for } G > 0 \tag{1}$$

$$f_v(v) = \left(\frac{\beta}{\alpha}\right) \times \left(\frac{v}{\alpha}\right)^{(\beta-1)} \times e^{-\left(\frac{b}{\alpha}\right)^{\beta}} \text{ for } 0 < v < \infty \tag{2}$$

2.1.2 Model of Wind Power

At time t, the output power [18] of the jth wind turbine for a particular velocity of wind is given as

$$\mathrm{P}_{wjt} = 0, \text{ for } v_{wt} < v_{in} \text{ and } \mathrm{P}_{wjt} = \mathrm{P}_{wrj} \times \left(\frac{v_{wt} - v_{in}}{v_r - v_{in}}\right)$$

$$\mathrm{P}_{wjt} = \mathrm{P}_{wrj} \times \left(\frac{v_{wt} - v_{in}}{v_r - v_{in}}\right), \text{ for } v_i \le v_{wt} \le v_r \tag{3}$$

$$\mathrm{P}_{wjt} = \mathrm{P}_{wrj}, \text{ for } v_r \le v_{wt} \le v_{out}$$

2.1.3 Model of Solar Power

At time t, the output power [19] from the kth PV solar plant is given as

$$\mathrm{P}_{PVkt} = \mathrm{P}_{srk} \times \left(\frac{G^2}{G_{std} R_c}\right), \text{ for } 0 < G < R_c \tag{4}$$

$$\mathrm{P}_{PVkt} = \mathrm{P}_{srk} \left(\frac{G}{G_{std}}\right), \text{ for } G \ge R_c$$

2.1.4 PV Power Probabilities

The PV power probability is the same as the related solar power irradiation probability, in terms of Eq. (5).

$$f_{PV}(\mathrm{P}_{PV}) = f_G(G) \tag{5}$$

2.1.5 Wind Turbine Power Probabilities

Wind power probabilities for discrete zones, i.e., for the first and third cases of (3), may be estimated using Eqs. (6) and (7) [15].

$$f_w(\mathrm{P}_w)|_{\mathrm{P}_W=0} = 1 - e^{-\left(\frac{v_{in}}{\alpha}\right)^{\beta}} + e^{-\left(\frac{v_{out}}{\alpha}\right)^{\beta}} \tag{6}$$

$$f_w(\mathrm{P}_w)|_{\mathrm{P}_W=\mathrm{P}_{Wr}} = -e^{-\left(\frac{v_{in}}{\alpha}\right)^{\beta}} - e^{-\left(\frac{v_{out}}{\alpha}\right)^{\beta}} \tag{7}$$

As in the second situation in Eq. (3), the probability of WT power in the uninterrupted zone may be calculated in Eq. (8).

$$f_w(\mathrm{P}_w) = \frac{\beta \times (v_r - v_{in})}{\alpha^{\beta} + \mathrm{P}_{wr}} \times \left[v_{in} + \frac{\mathrm{P}_w}{\mathrm{P}_{wr}} \times (v_r - v_{in})\right]^{(\beta-1)} \times e^{-\left(\frac{v_{in} + \frac{\mathrm{P}_w}{\mathrm{P}_{Wr}} \times (v_r - v_{in})}{\alpha}\right)^{\beta}} \tag{8}$$

2.2 Modelling Outage of Wind Turbine and Solar Power Plant

As a result of harsh climatic conditions, renewable energy sources are often driven out of service owing to the deterioration of their components and the inability to repair them. For any power system, the repairable forced outage rate is given as Eq. (9) [16].

$$\rho_{Repair} = \frac{F \times MTTR}{8760} \tag{9}$$

The component aging failure model typically follows the normal PDF throughout the service duration. The aging rate of failure is determined by Eq. (10).

$$\rho_{Aging} = \frac{1}{\sigma_{Norm} \times \sqrt{2 \times \Pi}} \times e^{-\frac{(\mathrm{T} - \mu_{Norm})^2}{2 \times \sigma_{Norm}^2}} \tag{10}$$

For a time period of Δt, by exponential distribution as Eq. (11), the weather-dependent failure model is modeled as follows:

$$\rho_{Weather} = 1 - e^{-\lambda \times \Delta t} \tag{11}$$

As a result, a multi-factor independent outage occurs, and the outage rate may be estimated using the union set idea. For any renewable unit, the forced outage rate can be given by Eq. (12).

$$\rho = \rho_{Repair} \cup \rho_{Aging} \cup \rho_{Weather} = \rho_{Repair} + \rho_{Aging} + \rho_{Weather} - \rho_{Repair} \times \rho_{Aging} - \rho_{Aging} \times \rho_{Weather} - \rho_{weather} \times \rho_{Repair} - \rho_{Repair} \times \rho_{Aging} \times \rho_{Weather} \tag{12}$$

2.3 Objective with Constraints

For optimal bidding, simultaneously total cost and emission are optimized considering every operational constraint. Total cost is the sum of the energy costs purchased from the grid, the fuel and operation costs of gas turbines, and the operation costs of solar PV plants and wind turbines during the entire time scale. Total emissions are the sum of emissions corresponding to the purchase of grid power and emissions from gas turbines.

2.3.1 Cost

As fuel costs rise, gas turbine output power increases quadratically. Solar PV and wind turbine operations include reserve expenses for overestimation of direct costs and penalties for underestimating dispatchable solar electricity and wind power, respectively. The total cost is the sum of the fuel cost of GT power, the cost of power purchased from the grid, and the operational cost of the PV solar plant and wind turbine [28–31].

$$F_C = \sum_{t=1}^{\mathrm{T}} \left[\sum_{i=1}^{\mathrm{N}_G} \left\{ \left(a_{Gi} + b_{Gi} \times \mathrm{P}_{Git} + c_{Gi} \times \mathrm{P}_{Git}^2 \right) \times S_{Git} \right\} + \left(cgrid_t \times \mathrm{P}_{grid,t} \right) + \sum_{j=1}^{\mathrm{N}_w} \left\{ d_{wj} \times \mathrm{P}_{wjt} + O_{wjt} \left(\mathrm{P}_{wjt} \right) + U_{wjt} \left(\mathrm{P}_{wjt} \right) \right\} \times S_{wjt} + \sum_{k=1}^{\mathrm{N}_{PV}} \left\{ d_{PVk} \times \mathrm{P}_{PVkt} + O_{PVkt} \left(\mathrm{P}_{PVkt} \right) + U_{PVkt} \left(\mathrm{P}_{PVkt} \right) \right\} \times S_{PVkt} \right] \tag{13}$$

where $S_{wjt} = \begin{cases} 1, & \rho_{wjt} < F_w \\ 0, & otherwise \end{cases}$ and $S_{PVkt} = \begin{cases} 1, & \rho_{PVkt} < F_{PV} \\ 0, & otherwise \end{cases}$

On dispatchable wind power, the overestimation reserve cost and the underestimation penalty cost are modeled, respectively, in Eqs. (14) and (15).

$$O_{wjt} \left(\mathrm{P}_{wjt} \right) = o_{wj} \times \int_{\mathrm{P}_{wjt}^{\min}}^{\mathrm{P}_{wjt}} \left(\mathrm{P}_{wjt} - y \right) \times f_w \left(y \right) dy \tag{14}$$

$$U_{wjt} \left(\mathrm{P}_{wjt} \right) = u_{wj} \times \int_{\mathrm{P}_{wjt}}^{\mathrm{P}_{wjt}^{\max}} \left(y - \mathrm{P}_{wjt} \right) \times f_w \left(y \right) dy \tag{15}$$

Reserve costs and penalties for underestimated dispatchable solar power costs are modeled in Eqs. (16) and (17), respectively.

$$O_{PVkt}\left(\mathrm{P}_{PVkt}\right) = o_{PVk} \times \int_{\mathrm{P}_{PVkt}^{\min}}^{\mathrm{P}_{PVkt}} \left(\mathrm{P}_{PVkt} - x\right) \times f_{PV}\left(x\right) dx \tag{16}$$

$$U_{PVkt}\left(\mathrm{P}_{PVkt}\right) = u_{PVk} \times \int_{\mathrm{P}_{PVkt}}^{\mathrm{P}_{PVkt}^{\max}} \left(x - \mathrm{P}_{PVkt}\right) \times f_{PV}\left(x\right) dx \tag{17}$$

2.3.2 Emission

The ambient greenhouse gases, such as SOx, NOx, and CO_2, produced by gas turbines are modeled separately. But, for evaluation purposes, the total emission of greenhouse gases is given as the sum of a quadratic function, while the total emission is the sum of emissions from gas turbines and emissions of power taken from the upstream grid.

$$F_E = \sum_{t=1}^{\mathrm{T}} \left[\sum_{i=1}^{\mathrm{N}_G} \left\{ \left(\alpha_{Gi} + \beta_{Gi} \times \mathrm{P}_{Git} + \gamma_{Gi} \times \mathrm{P}_{Git}^2\right) \times S_{Git} \right\} + \left(egrid_t \times \mathrm{P}_{grid,t}\right) \right] \tag{18}$$

2.3.3 Power Balance Constraint

The limit of power balance is depicted in Eqs. (19) and (20), which state that the power procured from the grid, GTs, WTs, PVs, and PSH units will be scheduled according to the load considering DRP. Assuming that, when load is curtailed due to DRP, at that time $LS_t = 0$, and when load is shifted to base load demand, at that time no load is curtailed.

$$\begin{aligned} &\mathrm{P}_{grid,t} + \sum_{i=1}^{\mathrm{N}_G} \left(\mathrm{P}_{Git} \times S_{Git}\right) + \sum_{j=1}^{\mathrm{N}_w} \left(\mathrm{P}_{wjt} \times S_{wjt}\right) + \sum_{k=1}^{\mathrm{N}_{PV}} \left(\mathrm{P}_{PVkt} \times S_{PVkt}\right) + \sum_{l=1}^{\mathrm{N}_{pump}} \mathrm{P}_{ghlt} \\ &\quad = \left(1 - DR_t\right) \times L_{Base,t} + Ls_t \; t \in \mathrm{T}_{gen} \end{aligned} \tag{19}$$

$$\begin{aligned} &\mathrm{P}_{grid,t} + \sum_{i=1}^{\mathrm{N}_G} \left(\mathrm{P}_{Git} \times S_{Git}\right) + \sum_{j=1}^{\mathrm{N}_w} \left(\mathrm{P}_{wjt} \times S_{wjt}\right) + \sum_{k=1}^{\mathrm{N}_{PV}} \left(\mathrm{P}_{PVkt} \times S_{PVkt}\right) - \sum_{l=1}^{\mathrm{N}_{pump}} \mathrm{P}_{phlt} \\ &\quad = \left(1 - DR_t\right) \times L_{Base,t} + Ls_t t \in \mathrm{T}_{pump} \end{aligned} \tag{20}$$

The transfer capacity of the line that connects the MG to the main grid limits the amount of power that can be procured from the upstream grid (Eq. (21)).

$$0 \le \mathrm{P}_{grid,t} \le \mathrm{P}_{grid}^{\max} \tag{21}$$

2.3.4 Pumped-Storage-Hydraulic (PSH) Unit Constraints

$$V_{res,l(t+1)} = V_{res,lt} + Q_{phlt}\left(\mathrm{P}_{phlt}\right), \; l \in \mathrm{N}_{pump}, \; t \in \mathrm{T}_{pump} \tag{22}$$

$$V_{res,l(t+1)} = V_{res,lt} - Q_{ghlt}\left(\mathrm{P}_{ghlt}\right), \; l \in \mathrm{N}_{pump}, \; t \in \mathrm{T}_{gen} \tag{23}$$

$$\mathrm{P}_{ghl}^{\min} \le \mathrm{P}_{ghlt} \le \mathrm{P}_{ghl}^{\max} \; l \in \mathrm{N}_{pump}, \; t \in \mathrm{T}_{gen} \tag{24}$$

$$\mathrm{P}_{phl}^{\min} \le \mathrm{P}_{phlt} \le \mathrm{P}_{phl}^{\max}\ l \in \mathrm{N}_{pump},\ t \in \mathrm{T}_{pump} \tag{25}$$

$$V_{res,l}^{\min} \le V_{res,lt} \le V_{res,l}^{\max}\ l \in \mathrm{N}_{pump},\ t \in \mathrm{T} \tag{26}$$

At the beginning and end, the volume of water in the top reservoir of the PSH unit is taken, and the net amount used by the PSH unit is equal to zero.

$$V_{res,l0} = V_{res,l\mathrm{T}} = V_{res,l}^{start} = V_{res,l}^{end} \tag{27}$$

$$Q_{net,spent,l} = Q_{spent,TOT,l} - Q_{pump,TOT,l} = \sum_{t\in \mathrm{T}_{gen}} Q_{ghlt}\left(\mathrm{P}_{ghlt}\right) - \sum_{t\in \mathrm{T}_{pump}} Q_{phlt}\left(\mathrm{P}_{phlt}\right) = 0 \tag{28}$$

2.3.5 Generation Limits of Gas Turbine

$$\mathrm{P}_{Gi}^{\min} \le \mathrm{P}_{Git} \le \mathrm{P}_{Gi}^{\max}\ i \in \mathrm{N}_{G},\ t \in \mathrm{T} \tag{29}$$

2.3.6 Ramp Rate Limits of Gas Turbine

$$\begin{aligned} &\mathrm{P}_{Git} - \mathrm{P}_{Gi(t-1)} \le UR_i, \quad i \in \mathrm{N}_{G},\ t \in \mathrm{T} \\ &\mathrm{P}_{Gi(t-1)} - \mathrm{P}_{Git} \le DR_i,\ i \in \mathrm{N}_{G},\ t \in \mathrm{T} \end{aligned} \tag{30}$$

$$\begin{cases} \left(\mathrm{T}_{on,i,(t-1)} - MUT_i\right) \times \left(S_{Gi(t-1)} - S_{Git}\right) \ge 0, i \in \mathrm{N}_{G}, t \in \mathrm{T} \\ \left(\mathrm{T}_{Off,i,(t-1)} - MDT_i\right) \times \left(S_{Git} - S_{Gi(t-1)}\right) \ge 0, i \in \mathrm{N}_{G}, t \in \mathrm{T} \end{cases} \tag{31}$$

3 Demand Side Management

Demand-side management (DSM) programs have numerous advantages, such as improving the power system's security, reducing costs, and so on. Strategic conservation, demand response, and so on are some of the types of programs. The DSM is modeled using time-of-use (TOU) software [21], which fixes the net load demand. Off-peak or less expensive times are used to shift some demand away from peak times. Consequently, the load curve flattens, and the probable operating costs fall. Using Eq. (32) as a starting point, the TOU program numerical model is restricted by Eqs. (33)–(36).

$$L_t = (1 - DR_t) \times L_{Base} + L_{st} \tag{32}$$

$$\sum_{t=1}^{\mathrm{T}} L_{st} = \sum_{t=1}^{\mathrm{T}} DR_t \times L_{Base,t} \tag{33}$$

$$L_{Inc_t} = Inc_t \times L_{Base,t} \tag{34}$$

$$DR_t \le DR^{\max},\ t \in \mathrm{T} \tag{35}$$

$$Inc_t \le Inc^{\max},\ t \in \mathrm{T} \tag{36}$$

4 Non-Dominated Sorting Genetic Algorithm-II

The non-dominated sorting genetic algorithm (NSGA) was developed by Deb et al. [23] to cope with multi-objective optimization algorithms. Non-domination is used to grade solutions, while fitness distribution is used to control diversity. Srinivas et al. [24] pioneered the non-dominated sorting genetic algorithm II, which gives a more effective solution in terms of fitness distribution parameters than its predecessor. Because of space restrictions, NSGA-complete II's description is not provided here. The flow chart of NSGA-II is demonstrated in Fig. 1.

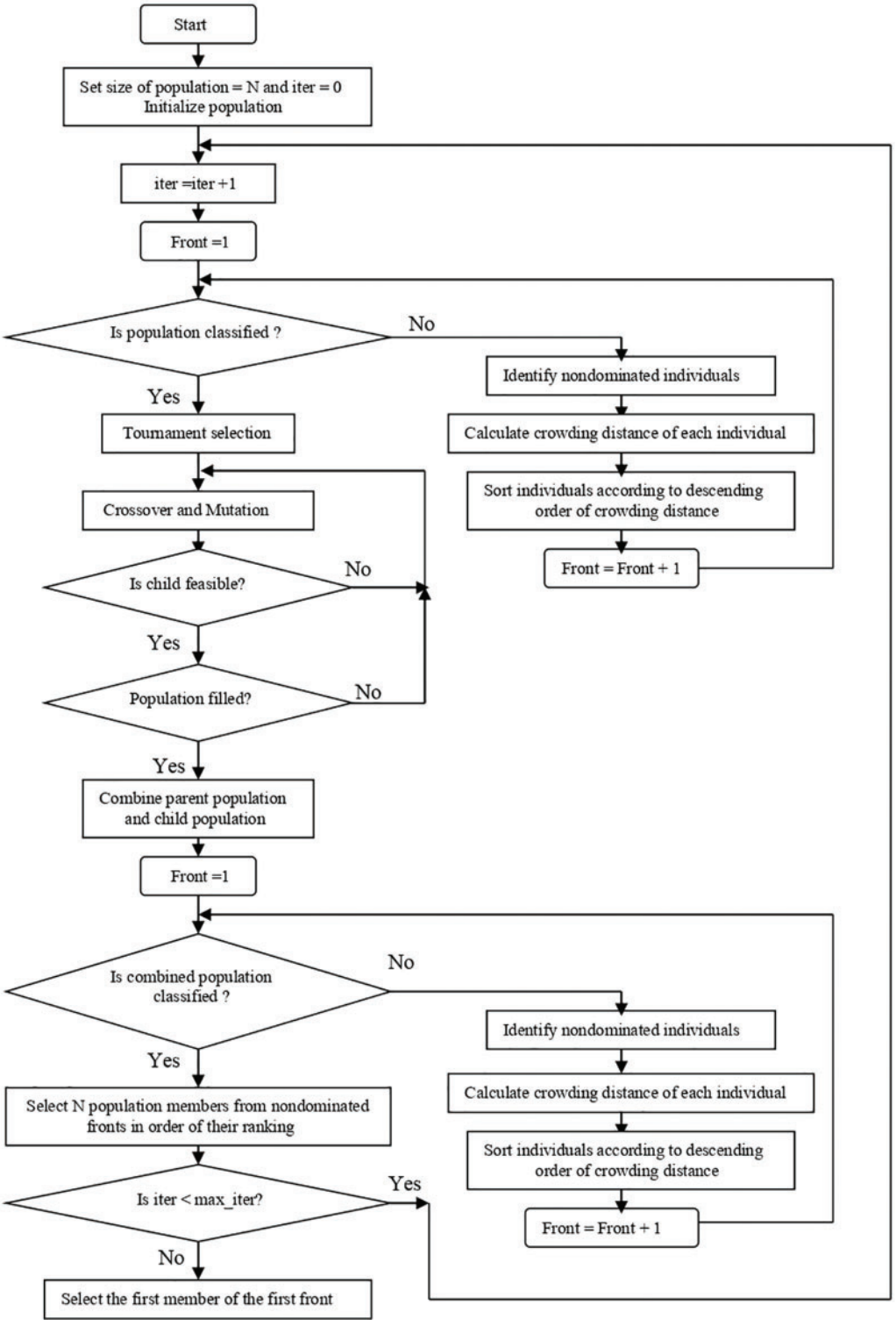

Figure 1: Flowchart of NSGA-II

5 Simulation Results

The proposed NSGA-II-based day-ahead optimal bidding strategy for MG based on economic environmental dispatch (EED) with DRP considering outages of intermittent renewable energy sources is performed using numerical simulation. Simulation outcomes of the test system are used to match the efficacy of the suggested NSGA-II with strength pareto evolutionary algorithm 2 (SPEA 2) [25]. Tables A1–A3 in Appendix A present the data for the grid-connected MG model's three gas turbines, one solar PV unit, one wind turbine, and one PSH unit. Table A4 shows the predicted loads and prices of power for the next 24 h, a day in advance. As a result of DSM, 15% of the load of the 16th and 17th h and 20% of the 19th h load were moved. The emission of grid electricity is assumed to be 50 kg per MWh. The following features describe the PSH plant: Generating mode: Q_{ght} is positive when generating, P_{ght} is positive and $0 \leq P_{ght} \leq 6$ MW, $Q_{ght}(P_{ght}) = 4 + 2P_{ght}$ acre-ft/hr.

Pumping mode: Q_{pht} is negative when pumping; P_{pht} is negative and $-6 < P_{pht} \leq 0$ MW, $Q_{pht}(P_{pht}) = -12$ acre-ft/h with $P_{pht} = -6$ MW.

Operating limitations: During pumping, the pumped hydro plant will be allowed to operate at a maximum power level of around 6 megawatts. During the first 24 h, the reservoir must be 160 acre-feet deep. Without taking spillage into account, the water inflow rate is ignored.

Figs. 2i and 2ii show the upper and lower projected limits for solar irradiation and wind velocity, respectively. Fig. 2 shows a rapid variation in the velocity of the wind at 16 o'clock (Fig. 2ii). High winds cause turbulent weather, which in turn causes renewable energy units to fail. As shown in Fig. 2, weather-dependent historical data may be used to estimate the failure rates of PV and WT units. Fig. 2iv depicts the comparable forced outage rates for those units. There are large failure rates for PV systems in the 16th and 17th h, as can be shown in Fig. 2iv. The WT unit has high failure rates in the 16th to 18th h. For PV and WT unit repairmen, the 17th or 18th h is necessary.

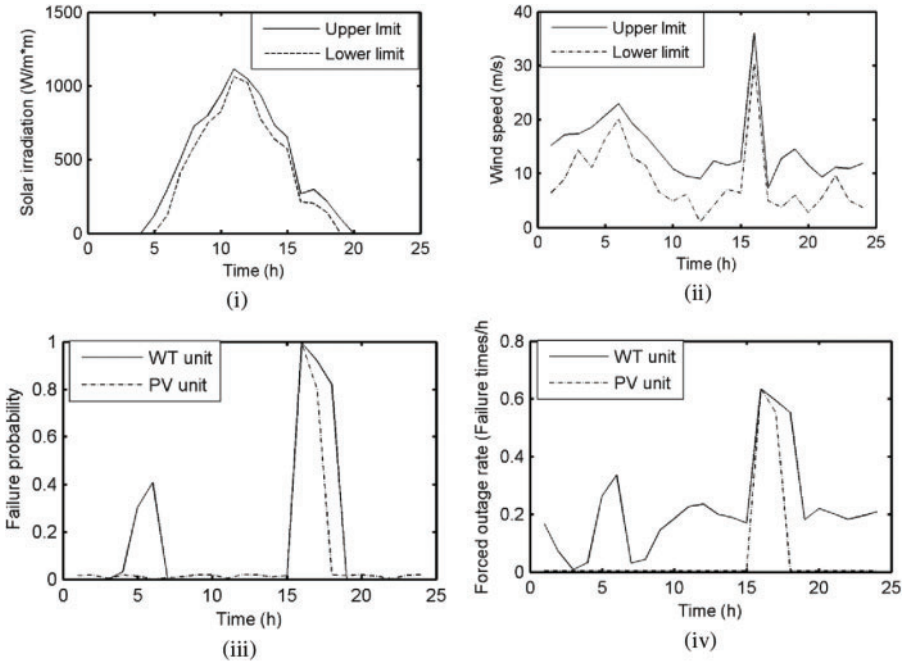

Figure 2: (i) Forecast limits of solar irradiation. (ii) Upper and lower forecast limits of wind speed. (iii) Failure probabilities (λ) for PV and WT. (iv) Forced outage rates of PV and WT units

The two opposing criteria are the total cost and the total amount of emissions. Each goal function, such as total cost and total emission, is reduced using a real-coded evolutionary algorithm in order to explain the relationships between the objective functions (RCGA). Using these parameters, the population size, the maximum number of iterations, the crossover, and the mutation probabilities are all set to 100, 200, 0.9, and 0.02.

NSGA-II has been used to simultaneously optimize both the total cost and the total emission goals. SPEA 2 has helped as a reference point in resolving this issue.

SPEA 2 and NSGA-II have a population size of 20, 30, 0.9, and 0.2, respectively, for crossover and mutation probabilities.

Electricity generated from gas turbines, wind, solar, and pumped storage, as well as power obtained from the upstream grid, is summarized in Table 1. In addition, Table 2 presents the hourly generation (MW) schedule acquired from emission dispatch. Data on the generation of gas turbine, wind, solar, and pumped storage, as well as electricity obtained from the upstream grid through economic emission dispatch, are presented in Tables 3 and 4 accordingly. Economic dispatch, emission dispatch, and economic emission dispatch all contribute to the overall cost and total emissions in Table 5. Figs. 3i and 3ii show the convergence characteristics of costs and emissions. Fig. 3iii shows, for instance, the distribution of the 20 non-dominated solutions obtained by NSGA-II and SPEA2 in their most recent iteration, which was derived by occurring as the result of cost and emission objectives.

Table 1: Hourly generation (MW) schedule acquired from economic dispatch

Hour	P_{G1}	P_{G2}	P_{G3}	P_{w}	P_{PV}	P_{gh}	P_{grid}
1	0.6298	0	1.5639	5.8212	0	−6.0000	12.9852
2	0.8553	3.0453	0.7363	3.7275	0	−6.0000	14.6356
3	0.3991	1.0051	0.8399	6.0000	0	−6.0000	16.7560
4	0.6081	1.3772	1.6879	6.0000	0	−6.0000	19.3268
5	0.4880	0.2047	1.9993	6.0000	0.1923	−6.0000	28.8158
6	1.9216	0.7481	2.7325	6.0000	0.8348	−6.0000	24.3881
7	1.5856	0.3667	0	6.0000	2.3992	−6.0000	24.6485
8	0.1625	1.9725	0.3555	5.7430	3.4953	−6.0000	22.2711
9	0.5190	1.1200	3.3573	2.9220	3.9706	2.3230	20.2882
10	0.8907	2.6495	1.5506	4.0779	4.5148	5.3246	8.9919
11	0.0170	1.4556	0.5235	2.9853	5.3980	5.2082	13.4123
12	0	0.0240	4.2554	3.2272	5.1496	1.2458	20.0979
13	0.3012	0	0.2509	3.6931	4.1066	3.3795	17.7686
14	2.2093	1.0051	0.9918	3.6435	3.4621	5.7353	26.9530
15	1.6945	1.4396	0.1913	2.0145	2.9754	2.2626	20.9221
16	0.3881	0.7093	2.4411	0	0	6.0000	22.7616
17	0.7696	1.8868	1.4992	0	0	3.1149	24.6046
18	2.2199	2.6392	1.0943	0	0.7651	6.0000	29.2816
19	3.1803	2.0358	3.7213	3.5852	0.0101	2.7308	22.7366
20	1.6180	2.9112	4.3674	3.6505	0	4.6711	26.7818
21	2.2493	3.4694	4.8920	2.5150	0	−6.0000	29.8743
22	1.2593	2.3805	0.3604	3.8269	0	−6.0000	22.1729

(Continued)

Table 1 (continued)

Hour	P_{G1}	P_{G2}	P_{G3}	P_w	P_{PV}	P_{gh}	P_{grid}
23	1.6118	2.5635	0.8152	4.0647	0	−6.0000	24.9448
24	0.3996	0.4968	2.5094	3.3909	0	−6.0000	23.7034

Table 2: Hourly generation (MW) schedule acquired from emission dispatch

Hour	P_{G1}	P_{G2}	P_{G3}	P_w	P_{PV}	P_{gh}	P_{grid}
1	7.0000	8.0000	1.1149	4.2348	0	−6.0000	0.6503
2	6.1038	4.2514	4.4232	3.9685	0	−6.0000	4.2530
3	7.0000	4.8154	6.0059	6.0000	0	−6.0000	1.1788
4	3.9615	5.5252	10.0000	6.0000	0	−6.0000	3.5133
5	7.0000	8.0000	8.3917	6.0000	0.2820	−6.0000	8.0263
6	4.1579	7.7078	6.9339	6.0000	1.1555	−6.0000	10.6700
7	7.0000	8.0000	10.0000	6.0000	2.1760	−6.0000	1.8240
8	3.3406	4.4722	7.9446	6.0000	3.2179	−6.0000	9.0247
9	0	4.4199	6.4004	5.3569	3.9839	6.0000	8.3390
10	3.6391	8.0000	10.0000	1.7040	4.5179	0	0.1390
11	0	5.7708	8.2316	2.9397	5.4283	6.0000	0.6297
12	3.3376	8.0000	10.0000	0.1225	5.2158	6.0000	1.3240
13	5.0748	5.4475	8.7944	3.2667	4.2871	0	2.6295
14	3.3861	8.0000	10.0000	3.7343	3.6557	0	15.2239
15	7.0000	6.7643	7.0934	3.1759	2.9030	0	4.5635
16	5.1998	8.0000	10.0000	0	0	6.0000	3.1002
17	7.0000	4.2384	6.1245	0	0	6.0000	8.5121
18	6.7873	8.0000	10.0000	0	0.7848	6.0000	10.4279
19	7.0000	7.1155	7.6116	1.6464	0.0193	6.0000	8.6072
20	4.4799	8.0000	4.3326	4.3861	0	6.0000	16.8014
21	7.0000	5.7954	6.5600	3.0305	0	−6.0000	20.6140
22	5.9080	8.0000	10.0000	3.6751	0	−6.0000	2.4168
23	7.0000	4.8374	9.8673	1.3874	0	−6.0000	10.9079
24	5.4220	8.0000	9.8645	4.4821	0	−6.0000	2.7314

Table 3: Hourly generation (MW) schedule acquired from EED using NSGA-II

Hour	P_{G1}	P_{G2}	P_{G3}	P_w	P_{PV}	P_{gh}	P_{grid}
1	2.9849	3.3890	6.0376	5.3880	0	−6.0000	3.2004
2	4.3916	4.8276	4.7287	6.0000	0	−6.0000	3.0521
3	5.5260	4.2543	5.5066	6.0000	0	−6.0000	3.7130

(Continued)

Table 3 (continued)

Hour	P_{G1}	P_{G2}	P_{G3}	P_{w}	P_{PV}	P_{gh}	P_{grid}
4	3.7725	1.6378	4.6157	5.7529	0	−6.0000	13.2211
5	5.3743	2.1891	3.8308	6.0000	0.5194	−6.0000	19.7865
6	5.7943	5.9921	7.5277	6.0000	1.4583	−6.0000	9.8526
7	4.6254	6.0212	8.6737	6.0000	2.1887	−6.0000	7.4911
8	3.3167	3.9214	4.1157	6.0000	3.4748	−6.0000	13.1714
9	3.7432	5.6613	4.8407	3.9216	3.9872	2.9205	9.4256
10	1.1587	5.1351	1.8917	3.1512	4.1462	2.0266	10.4904
11	4.2170	4.1247	3.0509	2.6654	5.3866	4.0886	5.4669
12	3.3202	5.7683	6.3407	1.8956	5.1213	4.0920	7.4619
13	1.9101	5.0711	3.8029	1.1529	4.4227	5.3794	7.7608
14	4.9169	4.0195	6.3225	4.5013	3.3649	5.7586	15.1164
15	2.7623	5.6823	5.1959	1.9308	3.2481	6.0000	6.6806
16	2.1534	3.6187	6.2732	0	0	0.8184	19.4364
17	4.2556	3.8879	5.5650	0	0	5.7746	12.3919
18	4.5558	5.1500	6.5900	0	0.9406	6.0000	18.7636
19	2.7147	3.1687	5.5892	6.0000	0.1918	2.5038	17.8318
20	2.7607	4.2326	5.5113	1.8022	0	2.6334	27.0598
21	5.1978	2.3587	7.0244	1.8975	0	−6.0000	26.5216
22	2.5099	2.6826	8.4443	4.1604	0	−6.0000	12.2028
23	1.6348	6.1588	6.7497	3.8893	0	−6.0000	15.5674
24	2.6016	4.9480	5.6753	2.3559	0	−6.0000	14.9193

Table 4: Hourly generation (MW) schedule acquired from EED using SPEA 2

Hour	P_{G1}	P_{G2}	P_{G3}	P_{w}	P_{PV}	P_{gh}	P_{grid}
1	2.5427	2.4507	6.7079	5.7131	0	−6.0000	3.5856
2	2.3406	1.9487	7.5644	4.2689	0	−6.0000	6.8774
3	3.6110	5.5991	7.3003	6.0000	0	−6.0000	2.4896
4	5.6085	6.2597	2.8790	6.0000	0	−6.0000	8.2528
5	1.8660	4.9910	6.7697	6.0000	0.0015	−6.0000	18.0719
6	3.7170	2.3154	2.3735	6.0000	0.8573	−6.0000	21.3618
7	3.2606	3.4488	2.3018	6.0000	2.5002	−6.0000	17.4885
8	1.7427	3.0117	6.5092	4.7685	3.6194	−6.0000	14.3486
9	1.9691	5.7996	5.8071	2.1872	3.8808	3.2319	11.6242
10	4.1763	2.8650	3.5324	3.1975	4.6041	5.6938	3.9310
11	3.1729	2.3437	2.6837	2.1978	5.4940	3.1735	9.9344
12	3.3695	2.3701	6.5418	1.8983	5.2217	4.8002	9.7984
13	5.3372	5.0548	4.4428	3.7490	4.6394	1.9723	4.3045
14	2.9497	2.6122	6.3042	3.9209	3.5155	4.8144	19.8830
15	2.3080	3.0905	6.2872	3.6466	2.8986	0.3914	12.8777

(Continued)

Table 4 (continued)

Hour	P_{G1}	P_{G2}	P_{G3}	P_w	P_{PV}	P_{gh}	P_{grid}
16	5.2098	4.5483	5.9327	0	0	6.0000	10.6092
17	2.3849	6.6198	7.9512	0	0	2.6639	12.2552
18	2.2529	7.4168	7.7712	0	0.8893	4.4687	19.2011
19	4.1608	5.2687	6.5545	3.5303	0.0175	5.6991	12.7692
20	4.4487	6.6452	7.5509	2.5236	0	5.0874	17.7442
21	2.3126	3.4898	7.9173	2.0801	0	−6.0000	27.2002
22	5.0339	5.1311	7.5146	3.8693	0	−6.0000	8.4510
23	2.8586	2.4976	8.0536	3.7064	0	−6.0000	16.8838
24	1.8391	3.8461	6.1609	4.2228	0	−6.0000	14.4311

Table 5: Comparison of performance

Type of problem and technique		Cost ($)	Emission (Kg)
Economic dispatch		63538	26394
Emission dispatch		217006	8910
EED	NSGA-II	130407	16098
	SPEA 2	131451	16286

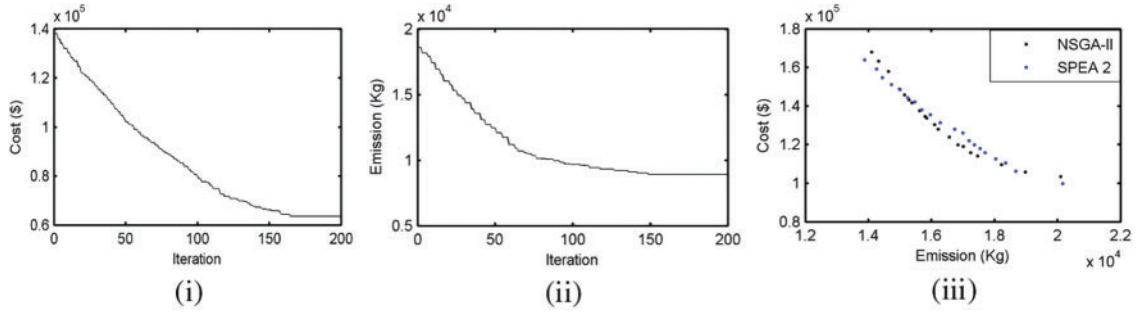

Figure 3: (i) Cost convergence characteristic. (ii) Emission convergence characteristic. (iii) Pareto-optimal front acquired from the last iteration

After analyzing the results and comparing the performances of NSGA-II with SPEA 2, it was found that the proposed NSGA-II method provides a better result in terms of cost and emissions compared to SPEA 2.

6 Conclusion

An NSGA-II-based day-ahead optimal bidding strategy for MG based on economic environmental dispatch is proposed with consideration of DRP under outage conditions and uncertainties about renewable energy sources. The uncertainty related to solar and wind units is modeled using lognormal

and Weibull probability distributions. TOU-based DRP is used, especially considering the time of outages along with the time of peak loads and prices, to enhance the reliability of MG and reduce costs and emissions. The cost obtained by using NSGA-II was 130407 US dollars, whereas for SPEA 2, it was 131451 US dollars. The emission obtained using NSGA-II was 16098 kg, whereas for SPEA 2, it was 16286 kg.

Acknowledgement: All authors acknowledge the support and cooperation of their respective institutions.

Funding Statement: The authors received no specific funding for this study.

Author Contributions: The authors confirm contribution to the paper as follows: study conception and design: Mousumi Basu, Chitralekha Jena, Baseem Khan, Ahmed Ali; data collection: Mousumi Basu, Chitralekha Jena, Baseem Khan, Ahmed Ali; analysis and interpretation of results: Mousumi Basu, Chitralekha Jena, Baseem Khan, Ahmed Ali; draft manuscript preparation: Mousumi Basu, Chitralekha Jena, Baseem Khan, Ahmed Ali. All authors reviewed the results and approved the final version of the manuscript.

Availability of Data and Materials: All data are presented in the paper.

Conflicts of Interest: The authors declare that they have no conflicts of interest to report regarding the present study.

References

1. Bazmohammadi, N., Madary, A., Vasquez, J. C., Mohammadi, H. B., Khan, B. et al. (2022). Microgrid digital twins: Concepts, applications, and future trends. *IEEE Access, 10,* 2284–2302.
2. Peng, Y., Lihong, M., Rong, F., Yafeng, L., Dan, Q. et al. (2023). Framework design and application perspectives of digital twin microgrid. *Energy Reports, 9(8),* 669–678.
3. Alshehri, J., Alzahrani, A., Khalid, M., Alismail, F. (2020). Optimal control of a microgrid with distributed renewable generation and battery energy storage. *IEEE Power & Energy Society Innovative Smart Grid Technologies Conference (ISGT)*, pp. 1–5. Washington, USA.
4. Lim, Y., Kim, H. M. (2014). Strategic bidding using reinforcement learning for load shedding in microgrids. *Computers & Electrical Engineering, 40(5),* 1439–1446.
5. Shayeghi, H., Sobhani, B. (2014). Integrated offering strategy for profit enhancement of distributed resources and demand response in microgrids considering system uncertainties. *Energy Conversion and Management, 87,* 765–777.
6. Nguyen, D. T., Le, L. B. (2014). Optimal bidding strategy for microgrids considering renewable energy and building thermal dynamics. *IEEE Transactions on Smart Grid, 5(4),* 1608–1620.
7. Xu, C., Huang, Y. (2023). Integrated demand response in multi-energy microgrids: A deep reinforcement learning-based approach. *Energies, 16,* 4769.
8. Liu, G., Xu, Y., Tomsovic, K. (2016). Bidding strategy for microgrid in day-ahead market based on hybrid stochastic/robust optimization. *IEEE Transactions on Smart Grid, 7(1),* 227–237.
9. Ferruzzi, G., Cervone, G., Monache, L. D., Graditi, G., Jacobone, F. (2016). Optimal bidding in a day-ahead energy market for micro grid under uncertainty in renewable energy production. *Energy, 106,* 194–202.
10. Wang, J., Zhong, H., Tang, W., Rajagopal, R., Xia, Q. et al. (2017). Optimal bidding strategy for microgrids in joint energy and ancillary service markets considering flexible ramping products. *Applied Energy, 205,* 294–303.

11. Nguyen, D. T., Le, L. B. (2015). Risk-constrained profit maximization for microgrid aggregators with demand response. *IEEE Transactions on Smart Grid, 6(1),* 135–146.
12. Pei, W., Du, Y., Deng, W., Sheng, K., Xiao, H. et al. (2016). Optimal bidding strategy and intramarket mechanism of microgrid aggregator in real-time balancing market. *IEEE Transactions on Industrial Informatics, 12(2),* 587–596.
13. Mehdizadeh, A., Taghizadegan, N. (2017). Robust optimisation approach for bidding strategy of renewable generation-based microgrid under demand side management. *IET Renewable Power Generation, 11(11),* 1446–1455.
14. Le, K. D., Golden, J. L., Stansberry, C. J., Vice, R. L., Wood, J. et al. (1995). Potential impacts of clean air regulations on system operations. *IEEE Transactions on Power Systems, 10(2),* 647–653.
15. Talaq, J. H., El-Hawary, F., El-Hawary, M. E. (1994). A summary of environmental/economic dispatch algorithms. *IEEE Transactions on Power Systems, 9(3),* 1508–1516.
16. Reddy, S. S., Bijwe, P. R., Abhyankar, A. R. (2015). Real-time economic dispatch considering renewable power generation variability and uncertainty over scheduling period. *IEEE Systems Journal, 9(4),* 1440–1451.
17. Li, W. Y. (2014). *Risk assessment of power systems: Models, methods, and applications*. USA: Wiley-IEEE Press.
18. Seguro, J. V., Lambert, T. W. (2000). Modern estimation of the parameters of the Weibull wind speed distribution for wind energy analysis. *Journal of Wind Engineering and Industrial Aerodynamics, 85(1),* 75–84.
19. Hetzer, J., Yu, D. C., Bhattarai, K. (2008). An economic dispatch model incorporating wind power. *IEEE Trans. on Energy Conversion, 23(2),* 603–611.
20. Liang, R. H., Liao, J. H. (2007). A fuzzy-optimization approach for generation scheduling with wind and solar energy systems. *IEEE T. Power Syst., 22(4),* 1665–1674.
21. Yousefi, A., Lu, H. H. C., Fernando, T., Trinh, H. (2013). An approach for wind power integration using demand side resources. *IEEE Transactions on Sustainable Energy, 4(4),* 917–924.
22. AlDavood, M. S., Mehbodniya, A., Webber, J. L., Ensaf, M., Azimian, M. (2022). Robust optimization-based optimal operation of islanded microgrid considering demand response. *Sustainability, 14(21),* 14194.
23. Deb, K., Agrawal, R. B. (1995). Simulated binary crossover for continuous search space. *Complex Systems, 9(2),* 115–148.
24. Srinivas, N., Deb, K. (1994). Multiobjective function optimization using nondominated sorting genetic algorithms. *Evolutionary Computation, 2(3),* 221–248.
25. Deb, K., Pratap, A., Agarwal, S., Meyarivan, T. (2002). A fast and elitist multiobjective genetic algorithm: NSGA-II. *Evolutionary Computation, 6(2),* 182–197.
26. Zitzler, E., Laumanns, M., Thiele, L. (2001). SPEA2: Improving the strength pareto evolutionary algorithm. *TIK Report*. Swiss Federal Institute of Technology (ETH).
27. Lei, X., Yu, H., Yu, B., Shao, Z., Jian, L. (2023). Bridging electricity market and carbon emission market through electric vehicles: Optimal bidding strategy for distribution system operators to explore economic feasibility in China's low-carbon transitions. *Sustainable Cities and Society, 94,* 104557.
28. Lei, X., Shang, Y., Shao, Z., Jia, Y., Jian, L. (2022). Grid integration of electric vehicles for optimal marginal revenue of distribution system operator in spot market. *Energy Reports, 8(13),* 1061–1068.
29. Hossein, N., Amin, S. (2020). Techno-economic assessment of combined power to hydrogen technology and hydrogen storage in optimal bidding strategy of high renewable units-penetrated microgrids. *Sustainable Energy Technologies and Assessments, 42,* 100832.
30. Navid, R., Yasin, P., Amirhossein, K. (2022). Economic-environmental risk-averse optimal heat and power energy management of a grid-connected multi microgrid system considering demand response and bidding strategy. *Energy, 240,* 122844.

31. Hosein, S., Taher, N., Mohsen, Z., Jamshid, A. (2022). Coordinated optimal bidding strategies methods of aggregated microgrids: A game theory-based demand side management under an electricity market environment. *Energy, 245,* 123205.
32. Adel, F. A., Khalid, A. A., Ahmad, M. A. (2024). A smart predict-and-optimize framework for microgrid's bidding strategy in a day-ahead electricity market. *Electric Power Systems Research, 228,* 110016.
33. Deepak, K., Sandeep, D., Yajvender, P. V., Rintu, K. (2022). Impact of optimal sized pump storage unit on microgrid operating cost and bidding in electricity market. *Journal of Energy Storage, 51,* 104373.

Appendix A

Table A1: Data of gas turbine

Parameter	1st GT	2nd GT	3rd GT	Unit
P_{Gi}^{max}	7	8	10	MW
P_{Gi}^{min}	0	0	0	MW
MUT_i	2	2	2	h
MDT_i	2	2	2	h
UR_i	4	4	5	MW
DR_i	4	4	5	MW
S_{Gi}	1	1	1	–
a_{Gi}	10.193	2.035	1.1825	$/h
b_{Gi}	105.18	60.28	65.34	$/MWh
c_{Gi}	62.56	44	44	$/MW^{2}h
α_{Gi}	2.655	15.443	29.038	Kg/h
β_{Gi}	−0.1618	−0.6415	−0.8969	Kg/MWh
γ_{Gi}	0.0705	0.1304	0.0622	Kg/MW^{2}h

Table A2: Data of PV unit

Parameter	Value	Unit	Parameter	Value	Unit
P_{PVk}	6	MW	*Life span*	15	Years
Irradiance at STC	1000	W/m^2	T	5	Years
Temperature at STC	25	°C	μ_{Norm}	13	–
$NOCT$	44	°C	σ_{Norm}	3	–
μ_{log}	5.2	–	F_{PV}	0.5	0.5
σ_{log}	0.6	–	d_{PVk}	6	$/MWh
F	33	Failure times/year	o_{PVk}	17	$/MWh
$MTTR$	63	Days	u_{PVk}	5	$/MWh

Table A3: Data of wind turbine unit

Parameter	Value	Unit	Parameter	Value	Unit
P_{wrj}	6	MW	*Life span*	20	Years
v_{in}	3	m/s	T	5	Years
v_r	14	m/s	μ_{Norm}	17	–
v_{out}	25	m/s	σ_{Norm}	4	–
α	9	–	F_w	0.5	–
β	2	–	d_{wj}	7	$/MWh
F	54	Failure times/year	o_{wj}	16	$/MWh
$MTTR$	96	Days	u_{wj}	5	$/MWh

Table A4: Day-ahead forecasted loads and forecasted grid price for consecutive 24 h

Hour	L_{Base}	c_{grid}	Hour	L_{Base}	c_{grid}
1	11.0	43.5	13	25.5	54.0
2	13.0	67.0	14	40.0	81.5
3	15.0	59.0	15	27.5	76.5
4	19.0	68.0	16	34.0	92.0
5	22.0	70.0	17	33.5	97.0
6	21.0	77.5	18	38.0	113.0
7	25.0	85.0	19	43.5	100.0
8	24.0	98.0	20	40.0	115.0
9	21.0	90.0	21	33.0	101.0
10	24.0	71.0	22	20.0	105.0
11	25.0	64.0	23	24.0	77.0
12	30.0	56.5	24	20.5	79.0